

GENERAL ARTICLE

Cytoplasmic TDP-43 is involved in cell fate during stress recovery

Youn-Bok Lee^{1,*}, Emma L. Scotter³, Do-Young Lee¹, Claire Troakes⁴, Jacqueline Mitchell¹, Boris Rogelj^{5,6,7}, Jean-Marc Gallo¹ and Christopher E. Shaw^{1,2,*}

¹Department of Basic and Clinical Neuroscience, Maurice Wohl Clinical Neuroscience, Institute of Psychiatry, Psychology and Neuroscience, Kings College, SE5 9NU London, UK, ²UK Dementia Research Institute Centre, Institute of Psychiatry, Psychology and Neuroscience, Maurice Wohl Clinical Neuroscience Institute, SE5 9RT London, UK, ³Centre for Brain Research, The University of Auckland, Auckland 1010, New Zealand, ⁴Basic and Clinical Neuroscience Department, Institute of Psychiatry, Psychology and Neuroscience, King's College, SE5 8AF London, UK, ⁵Department of Biotechnology, Jozef Stefan Institute, SI-1000 Ljubljana, Slovenia, ⁶Biomedical Research Institute BRIS, SI-1000 Ljubljana, Slovenia and ⁷Faculty of Chemistry and Chemical Technology, University of Ljubljana, SI-1000 Ljubljana, Slovenia

*To whom correspondence should be addressed at: Department of Basic and Clinical Neuroscience, Maurice Wohl Clinical Neuroscience, Institute of Psychiatry, Psychology and Neuroscience, Kings College, SE5 9NU London, UK. Tel: 0044 20 7848 6915; Email: younbok.lee@kcl.ac.uk (Y.-B. Lee); Tel: 0044 20 7848 5180; Fax: 0044 20 7848 5914; chris.shaw@kcl.ac.uk (C.E. Shaw)

Abstract

Transactive response DNA binding protein 43 (TDP-43) is an RNA processing protein central to the pathogenesis of amyotrophic lateral sclerosis (ALS) and frontotemporal dementia (FTD). Nuclear TDP-43 mislocalizes in patients to the cytoplasm, where it forms ubiquitin-positive inclusions in affected neurons and glia. Physiologically, cytoplasmic TDP-43 is associated with stress granules (SGs). Here, we explored TDP-43 cytoplasmic accumulation and stress granule formation following osmotic and oxidative stress. We show that sorbitol drives TDP-43 redistribution to the cytoplasm, while arsenite induces the recruitment of cytoplasmic TDP-43 to TIA-1 positive SGs. We demonstrate that inducing acute oxidative stress after TDP-43 cytoplasmic relocation by osmotic shock induces poly (ADP-ribose) polymerase (PARP) cleavage, which triggers cellular toxicity. Recruitment of cytoplasmic TDP-43 to polyribosomes occurs in an SH-SY5Y cellular stress model and is observed in FTD brain lysate. Moreover, the processing body (P-body) marker DCP1a is detected in TDP-43 granules during recovery from stress. Overall, this study supports a central role for cytoplasmic TDP-43 in controlling protein translation in stressed cells.

Introduction

Mislocalization of transactive response DNA binding protein 43 (TDP-43) from the nucleus to the cytoplasm has been identified as a pathogenic mechanism in amyotrophic lateral

sclerosis (ALS) and frontotemporal dementia (FTD) (1,2). As a DNA/RNA binding protein, TDP-43 shuttles continuously between the nucleus and the cytoplasm, while impairment of nuclear import depletes nuclear TDP-43 leading to cytoplasmic accumulation (3,4). Cytoplasmic TDP-43 inclusions are not

Received: March 19, 2021. Revised: May 22, 2021. Accepted: June 22, 2021

© The Author(s) 2021. Published by Oxford University Press. All rights reserved. For Permissions, please email: journals.permissions@oup.com

This is an Open Access article distributed under the terms of the Creative Commons Attribution Non-Commercial License (<http://creativecommons.org/licenses/by-nc/4.0/>), which permits non-commercial re-use, distribution, and reproduction in any medium, provided the original work is properly cited. For commercial re-use, please contact journals.permissions@oup.com

restricted to ALS/FTD cases but are commonly detected in other neurodegenerative diseases, including Alzheimer's and Parkinson's disease (5–10).

It has been proposed that cytoplasmic stress granules may be the site of initial TDP-43 aggregation which seed or nucleate cytoplasmic inclusions (11). Stress granules (SGs) are heterogeneous structures that harbour transcriptional and translational components, including mRNAs that accumulate in the nucleus or cytoplasm in cells under stress conditions such as heat shock, oxidative and osmotic shock (12). The principal function of SGs is to arrest steady-state translation, enabling the translation of specific stress response mRNAs, typically translated at low levels that promote cellular recovery. SGs preserve other non-essential mRNAs which, upon recovery from stress, resume translation (13). SGs are membrane-less organelles that are dynamic and move between polysomes and processing bodies (P-bodies) where translation-arrested mRNA can be degraded (14). The major components of SGs include T cell-induced antigen 1 (TIA-1), poly-A binding protein 1 (PABP1), ribosomal initiation complex 48S and small RNA processing components, which promote SG assembly through their prion-like low complexity domains in response to stress (15,16).

Many studies have reported that TDP-43 is recruited to SGs in response to oxidative stress (17–20). However, little is known about the role of aberrant cytoplasmic TDP-43 and related translational polyribosome assemblies under stress conditions other than oxidative stress. Here, we explored the effect of osmotic shock (sorbitol) and oxidative stress (arsenite) alone and combined, on TDP-43 cytoplasmic accumulation and polysome profiles. We find that cytoplasmic TDP-43 plays a central role in the control of translation in stressed cells.

Results

TDP-43 rapidly translocates to the cytoplasm following osmotic shock (sorbitol) compared with oxidative stress (arsenite)

In ALS/FTD, the nuclear protein TDP-43 is cleared from the nucleus and accumulates in the cytoplasm to form inclusion bodies (2); however, the drivers of TDP-43 mislocalization are not well understood. The progressive accumulation of TDP-43 in SGs in the cytoplasm could contribute to the mislocalization of TDP-43 in ALS/FTD. To test this hypothesis, SG inducers arsenite (oxidative stress) and sorbitol (osmotic stress) were applied to a neuronal cell line (SH-SY5Y) and TDP-43 distribution was monitored by immunofluorescence.

TDP-43 and T-cell restricted intracellular antigen-1 (TIA-1) are predominantly nuclear in unstressed SH-SY5Y cells (Fig. 1 Aa). One-hour incubation with arsenite (500 μ M) did not increase cytoplasmic TDP-43 levels compared with untreated controls. Although TIA-1-positive SG granules were detected in most arsenite-stimulated cells, these were rarely positive for TDP-43 (Fig. 1 Ac and b). Conversely, osmotic stress induced by sorbitol treatment (600 mM) caused a dramatic shift of TDP-43 and TIA-1 from nucleus to the cytoplasm (Fig. 1 Ad and b). This demonstrates that osmotic stress is more effective in translocating TDP-43 to the cytoplasm than oxidative stress.

To test the time course of TDP-43 distribution following osmotic shock, the intensity of cytoplasmic TDP-43 was measured every 15 min. Maximum cytoplasmic TDP-43 intensity was seen after 45 min incubation with sorbitol (Fig. 1 Ba). Fused in sarcoma (FUS) is another predominantly nuclear DNA/RNA binding protein and cytoplasmic FUS inclusions are associated with a subset of ALS/FTD (23). FUS is predominantly located in

the nucleus under resting conditions (Supplementary Material, Fig. S1A). Similar to TDP-43, FUS was not translocated to the cytoplasm or detected in TIA-1 positive cytoplasmic SG following oxidative stress induced by arsenite (Supplementary Material, Fig. S1B). FUS was however rapidly cleared from the nucleus following osmotic shock (sSupplementary Material, Fig. S1C and D).

To define the time course of TDP-43 and FUS relocalization to the cytoplasm by sorbitol, cytoplasmic fractions of SH-SY5Y cells were collected at 1-hour intervals following sorbitol treatment and analyzed by western blotting. Cytoplasmic levels of TDP-43, FUS and hnRNP1 were increased in a time-dependent manner following sorbitol treatment (Fig. 1 Bb). These results suggest that the sorbitol-mediated shift of nuclear proteins to the cytoplasm occurs rapidly and is not limited to TDP-43. A time-dependent increase in cytoplasmic TDP-43, FUS and hnRNP1 was also observed in HeLa (cervical cancer) cells following sorbitol incubation (Supplementary Material, Fig. S2A). However, other nuclear proteins (Sam-68 and hnRNP-U) did not show relocalization to cytoplasm (Supplementary Material, Fig. S2C). In addition, increased levels of insoluble TDP-43 were detected in SH-SY5Y cells incubated with arsenite or sorbitol for 30 min (Supplementary Material, Fig. S2Ba). TDP-43 insolubility was further increased by combining arsenite and sorbitol exposure. In contrast, there was no evidence that FUS became insoluble following osmotic or oxidative stress (Supplementary Material, Fig. S2Bb). These results demonstrate that sorbitol-induced cytoplasmic TDP-43 relocalization is not cell type-specific, and that insoluble TDP-43 is increased by both arsenite and sorbitol.

Next, we tested whether the stress signalling and cell death pathways were activated in parallel with TDP-43 cytoplasmic localization. Levels of phospho-eIF2a are known to increase in response to cellular stress and mediate a reduction in mRNA translation. Phosphorylation of eIF2a was increased after 1 h of sorbitol treatment, and gradually increased over 3 h in both HeLa and SH-SY5Y cells (Supplementary Material, Fig. S3). Levels of phosphorylated AKT1 and poly (ADP-ribose) polymerase (PARP) cleavage are known to reflect activation of the apoptotic pathway. Sorbitol treatment of SH-SY5Y and HeLa cells increased phosphorylated AKT1 and PARP cleavage, suggesting that the cells were undergoing apoptosis in response to osmotic shock (Supplementary Material, Fig. S3). Overall, these data provide evidence that cytoplasmic translocation of TDP-43 and FUS occurs in parallel with a reduction in translation (phosphorylation of eIF2a) and an increased in apoptosis (PARP cleavage) in response to osmotic shock by sorbitol.

Arsenite and sorbitol induce distinct ribosomal RNA profiles

Given that osmotic stress is known to induce translational stalling, we hypothesized that TDP-43 may be involved in the translational control of cytoplasmic RNA pools, including polysome-associated RNA. To test for interaction between the translational machinery and TDP-43, we used sucrose gradients to separate ribosomal fractions and characterized arsenite- and sorbitol-induced polysome profiles (Fig. 1C). We excluded the insoluble fraction by pre-centrifugation and used supernatants to prepare ribosomal fractions. The normal RNA profile obtained from the sucrose gradient gave the expected 260 nm absorbance profile for RNA associated with 40S, 60S and 80S ribosomal components and polysomes. Each fraction from the gradient was then immunoblotted to detect TDP-43, FUS and the 40S-ribosomal subunit protein, RPS-19 (Fig. 1 Ca).

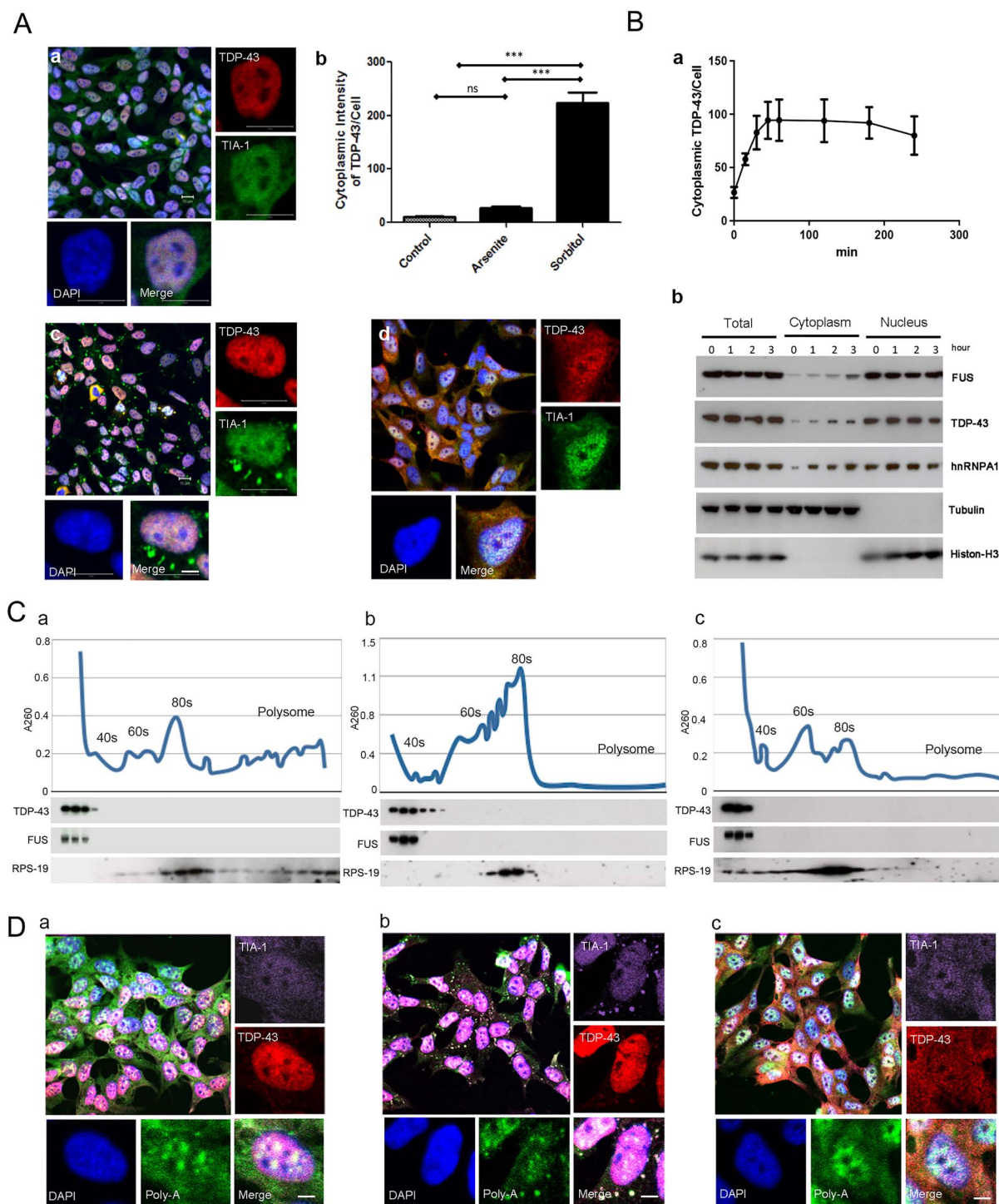


Figure 1. Nuclear TDP-43 is released to the cytoplasm by osmotic shock but not by oxidative stress. (A) Detection of TDP-43 redistribution following arsenite or sorbitol treatment. SH-SY5Y cells were untreated (a) or treated with either arsenite (500 μ M) for 1 h (c), or high-osmolarity sorbitol (600 mM) medium for 1 h (d). The cells were fixed and immunostained with anti-TIA-1 (green) and TDP-43 (red) antibodies to detect endogenous proteins by confocal microscopy. DAPI is used as a nuclear marker. Scale bars = 10 μ m. Cytoplasmic intensity of TDP-43 measured under arsenite and sorbitol stress ($P < 0.001$) (b). (B) The cytoplasmic intensity of TDP-43 was measured using an IN Cell™ Analyzer 1000. SH-SY5Y cells were cultured in 96 well plates and sorbitol was added. Images were captured at the indicated times at 15 min intervals (a). The captured images of the cytoplasm were segmented then the intensity of TDP-43 was analyzed using the IN Cell™ Analyzer 1000. The graph is the result of six experimental sets and presented as the mean \pm SEM. Western blot analysis of nuclear and cytoplasmic fractions from SH-SY5Y. FUS, TDP-43 and hnRNPA1 antibodies were used for detection (b). To ensure the absence of nuclear contamination in cytoplasmic fractions, tubulin (for cytoplasmic fraction) and histone H3 (for nuclear fraction) antibodies were used, and the data indicated that there was no cross contamination between fractions thus TDP-43 and FUS are released from the nucleus in response to osmotic stress. (C) Characterization of ribosomal RNA redistribution following oxidative and osmotic shock. SH-SY5Y cells were untreated (a) or treated with either (b) arsenite (500 μ M) or (c) sorbitol (600 mM) for 30 min and the lysates were separated by centrifugation in a 10–50% sucrose gradient. Each fraction was used for polysome profiling and analysis of TDP-43, FUS and ribosomal protein 19 (RPS-19) distribution by immunoblotting as indicated. (D) Double immunocytochemistry *in-situ* hybridization of SH-SY5Y cells untreated (a) or treated with (b) arsenite (500 μ M) or (c) sorbitol (600 mM) for 30 min. *In-situ* hybridization was used to detect the distribution of mRNA in the cytoplasm using an oligo dT probe to analyze the possibility of TDP-43 (red) sequestration into mRNA granules and SGs (TIA-1, purple), scale bar = 5 μ m.

In untreated SH-SY5Y cells, RPS-19 was undetectable in 40S subunit fractions, being found mainly in the 80S monosome and polysome fractions, where protein translation occurs. TDP-43 and FUS were both located in the RNA monomer region (Fig. 1 Ca), which indicates that they are not directly involved in regulating protein translation in the resting state. Oxidative stress induced by arsenite treatment resulted in polysome disruption. Both RNA and RPS-19 were shifted left, from the polysome to 80S monosome fractions, while TDP-43 was shifted right towards the 60S region (Fig. 1 Cb). In contrast, the location of FUS remained unchanged. These data suggest that TDP-43 may become associated with ribosomal subunit/RNA complexes in response to oxidative stress. With sorbitol treatment, similar to arsenite, polysomes were again completely disrupted. However, RNA shifted towards the 40S and 60S rather than 80S fractions (Fig. 1 Cc). TDP-43 and FUS remained in the monomer region, while RPS-19 accumulated in the monosome fraction (Fig. 1 Cc). This finding suggests that sorbitol treatment results in the dissociation of the 80S-ribosomal complex to 40S and 60S subunits.

Given our hypothesis that TDP-43 and FUS sequestration within the SG complex is important in the attenuation of mRNA translation during stress, we investigated whether polyadenylated mRNA (poly-A) was co-localized with TDP-43 and/or FUS in SGs. We performed *in-situ* hybridization using an oligo-dT (18 mer) probe to detect poly-A mRNAs prior to TDP-43 immunocytochemistry and confocal imaging. In the absence of stress, TDP-43 and TIA-1 are predominantly nuclear and poly-A positive mRNAs were evenly distributed between the nucleus and cytoplasm (Fig. 1 Da). Following arsenite stress, TIA-1 colocalized with cytoplasmic granules of poly-A mRNA while TDP-43 remained nuclear (Fig. 1 Db), suggesting that arsenite is not a strong inducer of TDP-43 export from the nucleus. In contrast, sorbitol induced TDP-43 cytoplasmic relocalization, however there was no evidence of TIA-1, TDP-43 and poly-A mRNA colocalizing in cytoplasmic SGs (Fig. 1 Dc). Taken together, these results indicate that arsenite potentially induced cytoplasmic stress granule formation, polysome disassembly and TDP-43 co-migration with ribosomal subunits, while sorbitol induced polysome disassembly and TDP-43 translocation from the nucleus to the cytoplasm.

TDP-43 is detected in the polysome fraction in a sequential cellular stress model and in FTLD brain tissues

Given that TDP-43 mislocalizes and co-migrates with ribosomal subunits in stressed cells, we investigated whether similar changes in TDP-43 distribution occur in the brains of frontotemporal lobar degeneration (FTLD) patients. We conducted sucrose gradient separation of TDP-43-positive FTLD and control brain tissue samples to characterize TDP-43 distribution and ribosomal RNA profiles (Fig. 2A). Control tissue samples showed a ribosomal RNA profile (260 nm) similar to that seen in SH-SY5Y cells (Fig. 2 Ad-e). In contrast, the RNA profile of FTLD brain lysate exhibited evidence of polysome disassembly (Fig. 2 Aa-c). Notably, in FTLD cases TDP-43 was detected in the polysome and monosome fractions, and RNA monomer region, whereas in controls TDP-43 was detected only in the RNA monomer region (Fig. 2A).

Given the distinct ribosomal RNA profiles seen with sorbitol- and arsenite-induced stress, together with their differential effects on TDP-43 subcellular localization (Fig. 1), we hypothesized that sequential activation of oxidative and osmotic stress

may better mimic the TDP-43 profile seen in FTLD patients. We therefore investigated the effects of various combinations of these stressors in SH-SY5Y cells (Fig. 2B). Because FTLD is characterized by cell death and the pathological aggregation and cleavage of TDP-43, we first examined the extent of apoptosis (caspase-3 regulated cleavage of PARP), and the cleavage of TDP-43. Neither acute arsenite nor sorbitol stress alone induced apoptosis; however, sequential exposure to both stressors in either order significantly increased cleaved PARP cleavage (Fig. 2 Ba-b). Allowing a 30-min recovery period after sorbitol stress prior to harvesting cells also resulted in a significant increase in PARP cleavage, as did recovery from the combinatorial stress models, although there was no significant increase in PARP cleavage following a 30-min recovery from arsenite treatment. Notably, the level of cleaved PARP present in cells treated with arsenite then sorbitol, followed by a 30-min recovery period, was significantly higher than that seen in any of the other stress combinations, thus this stress combination may result in a significant increase in cellular death compared with the other combinations. Importantly, TDP-43 showed a 32 kDa cleaved fragment in cells following arsenite then sorbitol and recovery, or sorbitol and recovery, thus TDP-43 cleavage may be intrinsically linked to the activation of the apoptotic pathway (Fig. 2 Bb). Conversely, we identified no change in FUS cleavage in any of the stress conditions, suggesting that TDP-43 cleavage is a more sensitive reporter of the severity of the stress response.

TDP-43 is found in TIA-1 and poly-A positive granules following sequential arsenite-sorbitol stress

Next, we used sucrose gradient separation to assess the ribosomal RNA profile of cells in the combinatorial stress models and examined the concomitant TDP-43 and FUS profiles (Fig. 2C). Sorbitol followed by arsenite dramatically increased the amount of 60S and 80S complexes while dissociating polysome (Fig. 2 Ca). Western blot analyses demonstrated a slight shift in TDP-43 distribution towards the 60S fractions (Fig. 2 Cb). In contrast, there was no change in FUS distribution in response to stress in this model. RPS-19 was detected mainly in the 60S and 80S regions. *In-situ* hybridization and immunocytochemistry demonstrated large poly-A positive granules that colocalized with TIA-1 and TDP-43 (Fig. 2 Cc). Conversely, FUS immunoreactivity was confined to the nucleus in response to this stress regime (Supplementary Material, Fig. S4A). These results show that sequential osmotic then oxidative stress results in TDP-43 sequestration into TIA-1 and poly-A positive SGs.

Reversing sequential stress (arsenite followed by sorbitol), we found a dramatic decrease in the amount of 60S ribosomal complexes (Fig. 2 Da), again with a small amount of TDP-43 identified in the 60S fractions and no change in FUS (Fig. 2 Db). Intriguingly, *in-situ* hybridization and immunocytochemistry demonstrated a lack of co-localization between SGs and cytoplasmic TDP-43, which was abundant in the cytoplasm but remained diffuse (Fig. 2 Dc). Similarly, FUS was detected within all TIA-1 and poly-A positive granules (Supplementary Material, Fig. S4B). Collectively, these findings provide a mechanism whereby TDP-43 is released into the cytoplasm in response to osmotic shock, which is subsequently recruited to SGs in response to oxidative stress.

Arsenite-sorbitol-recovery stress mimics TDP-43 distribution in ribosomal fractions from FTLD brain

To further explore the pathological significance of our sequential stress model, we investigated the effect of a 30 min recovery

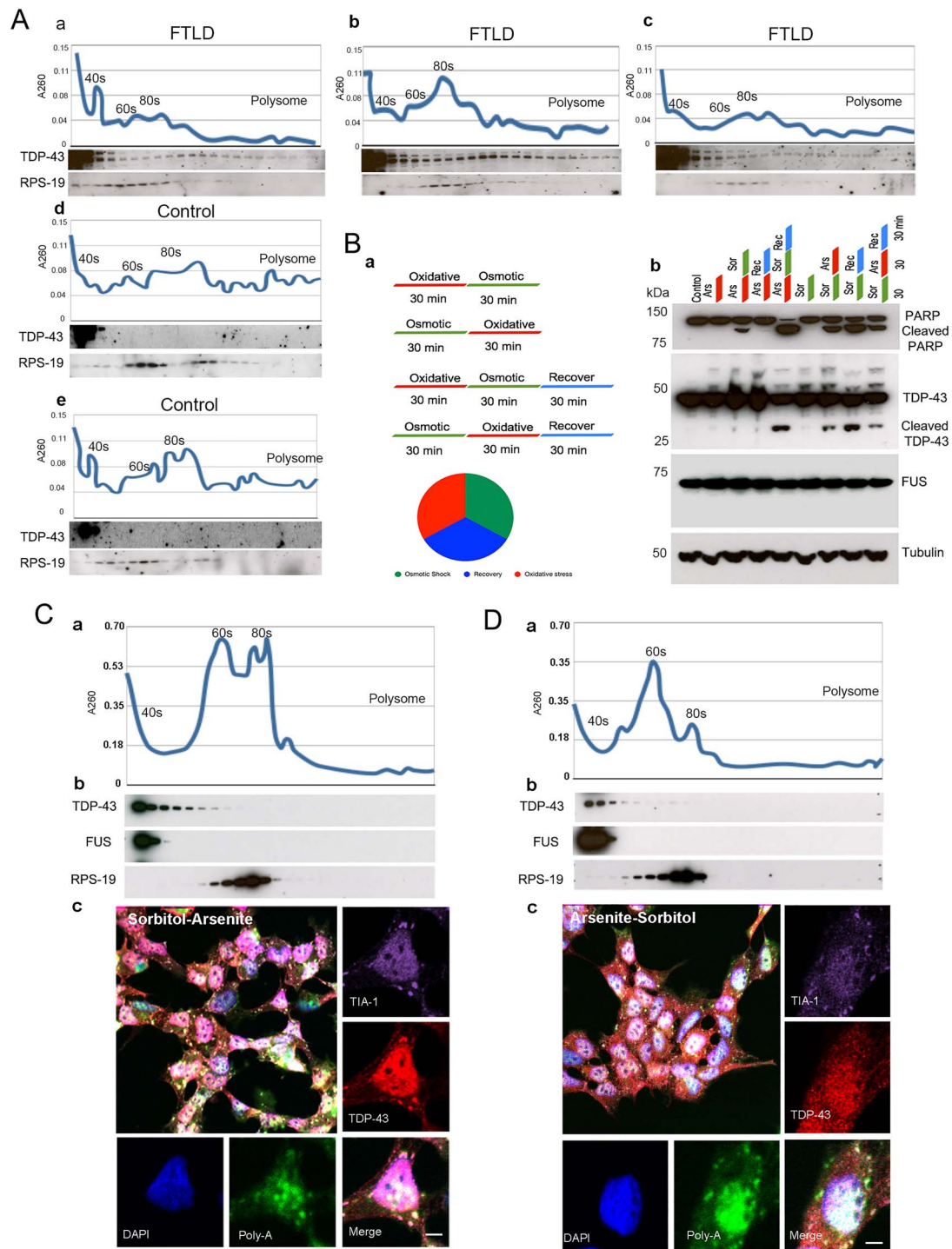


Figure 2. TDP-43 is sequestered into stalled ribosomes in FTLD patients and in a sequential stress cellular model. (A) Polysome fractionation from the cortex from FTLD patients, FTLD patient 1 (a), FTLD patient 2 (b), FTLD patient 3 (c) and control (d-e). Collected fractions from sucrose gradient (10–50%) were used for TDP-43 detection and RPS-19 used as a polyribosome marker. (B) Schematic diagram of sequential stress model. Following the two independent stress stimulants showed typical polysome separation, we used acute 30 min oxidative (arsenite) and osmotic (sorbitol) stress (a). This model used in reversed order including recovery. SH-SY5Y cells were incubated under sequential stress conditions then the cellular responses were assessed by PARP, TDP-43 and FUS. Tubulin was used as a loading control (b). (C) TDP-43 is found in SGs after sorbitol treatment followed by arsenite treatment. SH-SY5Y cells were treated with sorbitol (600 mM) for 30 min then the medium was replaced with medium containing arsenite (500 μ M) for another 30 min (S-A). The cells were lysed and separated on a 10–50% sucrose gradient (a). Each fraction was used for A 260 nm absorbance measurement for polysome profiling. Individual fractions were subjected to immunoblotting for TDP-43, FUS and ribosomal protein 19 (RPS-19) as indicated (b). *In-situ* hybridization was used to detect mRNA in the cytoplasm using an oligo dT probe to analyze the possibility of TDP-43 or FUS sequestration into mRNA granules (c). Scale bar = 5 μ m. (D) Reversed order; SH-SY5Y cells were incubated initially with arsenite for 30 min then the medium was replaced for medium containing sorbitol for further 30 min (A-S). The cells were lysed and separated on a 10–50% sucrose gradient. Each fraction was used for A 260 nm absorbance measurement for polysome profiling (a). Individual fractions were subjected to immunoblotting for TDP-43, FUS and ribosomal protein 19 (RPS-19) as indicated (b). *In-situ* hybridization was used to detect mRNA in the cytoplasm using an oligo dT probe to analyze the possibility of TDP-43 or FUS sequestration into mRNA granules (c). Scale bar = 5 μ m.

on polysomes (Fig. 3). Following recovery from sorbitol–arsenite stress, the relative size of the 80S and 60S peaks were reversed (Fig. 3 Aa), and TDP-43 was confined to the RNA monomer region (Fig. 3 Ab). TDP-43 sequestration to TIA-1 positive SGs was dramatically decreased during recovery, although some colocalization was still detectable (Fig. 3 Ac), in contrast to FUS, which remained confined to the nucleus (Supplementary Material, Fig. S5A).

Next, we assessed the effect of recovery from sequential arsenite then sorbitol. We observed a reduction in the 80S ribosomal RNA peak (Fig. 3 Ba), accompanied by the presence of TDP-43 throughout the monosome and polysome fractions (Fig. 3 Bb). This pattern of TDP-43 distribution was similar to that seen in brain samples from FTLN patients (Fig. 2), thus suggesting our arsenite–sorbitol sequential stress model followed by recovery may be relevant to disease. We noticed that cytoplasmic TDP-43 was now accumulated in small granules adjacent to TIA-1 SGs (Fig. 3 Bc). In contrast, FUS distribution throughout the sucrose gradient was, as before, not altered in response to the sequential stress activation then recovery, and FUS remained localized to the nucleus (Supplementary Material, Fig. S5B).

DCP1a colocalizes with TDP-43 following recovery from arsenite–sorbitol stress

We hypothesized that the small TDP-43-positive granules surrounding larger TIA-1 and poly-A positive SGs, identified during recovery from arsenite–sorbitol stress may be P-bodies. To test this hypothesis, we conducted immunocytochemical and co-immunoprecipitation studies using the P-body marker DCP1a (Fig. 3 Ca and Cc). DCP1a co-localized with TDP-43 granules adjacent to poly-A and TIA-1 positive SGs, suggesting TDP-43 is recruited to P-bodies following recovery from arsenite–sorbitol stress. To independently confirm TDP-43-DCP1a colocalization, we used immunoprecipitation to demonstrate a physical interaction between TDP-43 and DCP1a. Following recovery from arsenite–sorbitol stress, DCP1a was detected by TDP-43 immunoprecipitation (Fig. 3 Cb). Further studies investigating HA-tagged wild type or mutant (Q331K, M337V) TDP-43 in transfected cells demonstrated that DCP1a was pulled down by HA-tagged TDP-43 regardless of mutation status. We also showed that RNase treatment completely abolished TDP-43 and DCP1a interaction, suggesting that the binding of these two proteins is indirect, and requires the presence of RNA (Fig. 3 Cd). These findings support the hypothesis that poly-A mRNA in SGs may be recognized by DCP1a-TDP-43 P-bodies for further processing of the mRNA. This model may lend itself to further study of the P-body-stress granule interactions.

In conclusion, TDP-43 translocates to the cytoplasm in response to osmotic but not oxidative stress and is subsequently sequestered into cytoplasmic SGs following oxidative stress. Conversely, recovery from arsenite–sorbitol stress, results in a distribution of TDP-43, as defined by sucrose gradient profiling, similar to that seen in the brains tissues from FTLN patients. Thus, sequential stress paradigms may provide a better model to explore mechanistic aspects of ALS and FTD pathophysiology. Moreover, the switching from oxidative to osmotic stress, and events during the subsequent recovery period may play a crucial role in the deposition and processing of TDP-43, which may in turn be involved in the onset or progression of disease.

Discussion

The RNA-binding proteins TDP-43 and FUS are central to the pathogenesis of the vast majority of cases of the neurodegenerative disorders ALS and FTD. These proteins have multiple roles in the regulation of RNA splicing, exon skipping and the processing of noncoding RNA (21,22). The sequestration of TDP-43 into cytoplasmic inclusion bodies and loss of nuclear function of TDP-43 contribute to the death of affected neurons (1). TDP-43 is recruited to cytoplasmic SG, where untranslated mRNAs are sequestered when cells undergo oxidative stress (11). FUS is also recruited to SGs due to ALS-linked mutations in the nuclear localization signal (23).

The RNA-protein granules formed under stress, SG represent a system for cellular resistance to challenging environmental conditions such as oxidative and osmotic stress (24–28). This cellular buffering system is particularly important for neurons which have little capacity for regeneration and utilize neuro-transmission systems that continuously generate neuro-toxic reactive oxygen species (29–31). However, the mechanism by which nuclear TDP-43 re-locates to the cytoplasm and is recruited to SGs has yet to be elucidated.

Here we show that osmotic shock and oxidative stress have several distinct effects on TDP-43 and FUS. Osmotic stress more efficiently clears TDP-43 from the nucleus than oxidative stress, which on its own produces robust stress granules that are largely devoid of TDP-43. Osmotic shock induced robust cytoplasmic translocation of FUS similarly to TDP-43 as has previously been reported (27). However, the role of these two stressors is controversial for the recruitment of TDP-43 to SGs and may depend on the cell type and stress applied (17).

In an attempt to model TDP-43 recruitment to SGs, we applied osmotic and oxidative stress singly, sequentially and reverse order. Only the sequential exposure of cells to oxidative then osmotic stress resulted in abundant TDP-43 in the cytoplasm (Fig. 2D). Recovery from arsenite–sorbitol stimulation showed TDP-43 in the polysome fraction (Fig. 3 Bb). This coincided with an increased level of cleaved PARP (Fig. 2B). Supporting this, the cytoplasmic translocation of TDP-43 paralleled the translational stalling caused by eIF2a phosphorylation. Similar studies have also reported that TDP-43 is involved in translational stalling, which associated with stress (32,33). In contrast, recovery from sequential sorbitol–arsenite stimulation did not show TDP-43 in ribosomal fractions (Fig. 3 Aa-b). These results imply that cytoplasmic TDP-43 recruitment to polysomes increases cellular toxicity during recovery from the stress.

Moreover, our data suggest that TDP-43 is not involved in regulating protein translation in unstressed SHSY5Y cells, in which TDP-43 was found in the non-translating regions (monosome) of sucrose gradient profiles (Fig. 1C). Similar results were reported by Higashi *et al.* (32) who showed that TDP-43 was found in lower density in ribosomes. However, we demonstrated that FTLN brain lysates are enriched in monosomes and that TDP-43 is detected across the monosome and polysome fractions, implying an association between TDP-43 and stalled translational complexes. Importantly, recovery from sequential arsenite then sorbitol stress in SH-SY5Y cells recapitulated the co-elution of TDP-43 with monosome and polysome fractions from FTLN brain tissues, identifying this stress paradigm as a potential model of disease.

Recovery from oxidative stress followed by osmotic shock produced small TDP-43 positive foci that were surrounded by TIA-1 positive SGs (Fig. 3C). We speculated whether these TDP-43 foci were part of processing bodies (P-bodies), which are

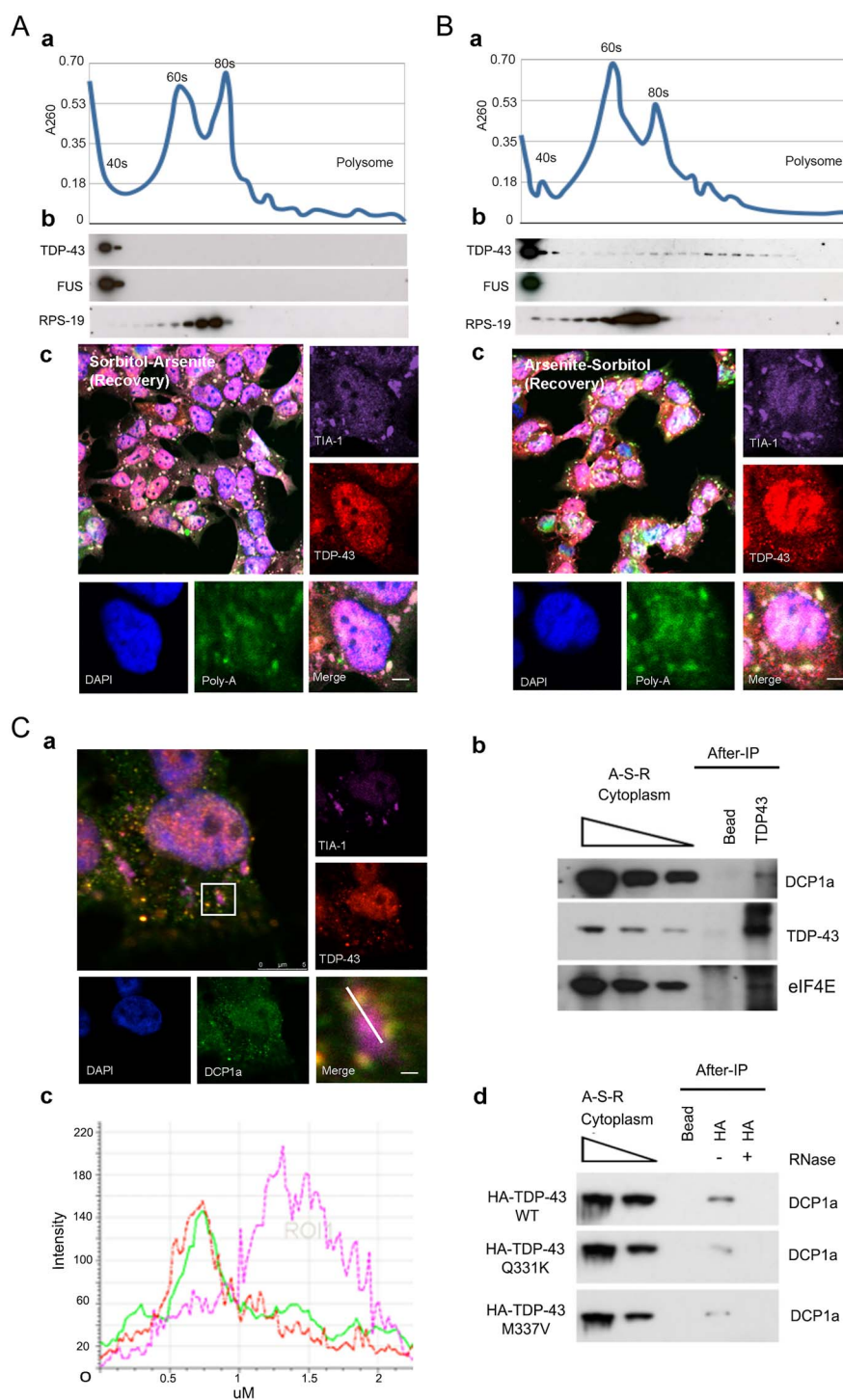


Figure 3. Recovery from sequential stress mimics TDP-43 sequestration in stalled-ribosomes. (A) SH-SH5Y cells were treated with sorbitol for 30 min then the medium was replaced with medium containing arsenite for another 30 min (S-A). Cells were then changed to normal medium to allow recovery for 30 min before being lysed and fractionated using 10–50% sucrose gradient centrifugation. Each fraction was used for A 260 nm absorbance measurement for polysome profiling (a). Individual fractions were analyzed by immunoblotting for TDP-43, FUS and ribosomal protein 19 (RPS-19) as indicated (b). *In-situ* hybridization was used to detect mRNA in the cytoplasm using an oligo dT probe to track the possibility of TDP-43 or FUS sequestration into mRNA granules (c). (B) SH-SY5Y cells were incubated initially with arsenite (500 μ M) for 30 min then the medium was replaced with medium containing sorbitol (600 mM) for 30 min (A-S). The medium was then changed to normal medium to allow recovery for 30 min. Cells were lysed and separated using 10–50% sucrose gradient centrifugation. Each fraction was used for A 260 nm absorbance measurement for polysome profiling (a). Individual fractions were analyzed by immunoblotting for TDP-43, FUS and ribosomal protein 19 (RPS-19) as indicated (b). *In-situ* hybridization was used to detect mRNA in the cytoplasm using an oligo dT probe to track the possibility of TDP-43, FUS sequestration into mRNA granules (c). (C) Cytoplasmic TDP-43 is recruited into DCP1a-positive granules during recovery from sequential stress (arsenite–sorbitol–recovery). TDP-43 (red), DCP1a (green), DAPI (Blue) and Tia-1 (purple), respectively (a). Scale bar = 5 μ m. Cells were lysed and immunoprecipitation performed with a TDP-43 antibody for DCP1a and eIF4E (b). Densitometry analysis of TDP-43 and DCP1 granules. Purple represents TIA-1, green represents DCP1a and red represents TDP-43 granule measured across the white line on the merged image (c). HA-tagged wild-type TDP-43 were used for cytoplasmic fractionation and performed immunoprecipitation using HA antibody for the detection of DCP1a (d). Cell lysates of (HA-TDP-43 wild-type, HA-TDP-43-Q331K, HA-TDP-43-M337V) were treated with RNase then used for immunoprecipitation.

primarily involved in translation repression and mRNA decay. Convergent studies from several laboratories have shown that P-bodies contain proteins involved in mRNA degradation including the de-capping enzymes DCP1a, Lsm, and the exonuclease XRN1 (34,35). We discovered that small TDP-43 foci are positive for DCP1a and interact with eIF4E (Fig. 3C), implying TDP-43 involvement in mRNA degradation (DCP1a) and protein translation (eIF4E) during the recovery process. Liu *et al.* (20) observed that there was close contact of TDP-43 with P-bodies under arsenite stress. Our assumption is that TDP-43 could be sequestered to P-bodies during the recovery period after sequential stimulation by the two stressors, arsenite and sorbitol.

Our hypothesis is that TDP-43 redistribution and aggregation is caused by repeated cycles of osmotic and oxidative stress and recovery. This recurring combination of stressors is consistent with evidence from epidemiological and theoretical modelling studies that multiple environmental 'hits' contribute to the pathophysiology of ALS and FTD in a multi-step process (36).

Materials and Methods

Cell culture, stressors and transfection

SH-SY5Y cells were obtained from ECACC and cultured in Ham's F12: DMEM (1:1), 2 mM Glutamine and 10% Foetal Bovine Serum (FBS). Cells were exposed to 500 μ M sodium arsenite or 600 mM sorbitol as indicated for each experiment. For immunofluorescence, cells were grown on coverslips and plasmids were transfected using lipofectamine 2000 transfection reagent (Invitrogen) according to the manufacturer's instructions. HA tagged TDP-43 wild type, Q331K and M337V were cloned into lentivirus shuttle plasmid by gateway cloning.

Immunocytochemistry

Cells were fixed with 4% paraformaldehyde in phosphate buffered saline for 15 min, permeabilized with 0.1% Triton X-100 for 5 min and non-specific binding sites were blocked with 10% normal donkey serum solution (Sigma). Overnight incubation was performed with primary antibodies to TDP-43, FUS, TIA-1 and DCP1a in blocking solution at 4°C. Dylight-conjugated secondary antibodies were used for detection and nuclei were visualized by 4'-6-diamidino-2-phenylindole (DAPI) staining (Sigma). Coverslips were mounted in Fluorsave (Calbiochem, USA) and imaging was performed using a Zeiss Axiovert 200M confocal laser scanning microscope (Carl Zeiss Ltd, Hertfordshire, UK) with C-apochromat 63x/1.2 water immersion objective and LSM 510 SP2 software version 3.2. The 96 well plate Images were acquired using IN Cell™ Analyzer 1000 (GE Healthcare).

In-situ hybridization of poly-A RNA

Cells at sub-confluence were prepared for fluorescence *in-situ* hybridization by rinsing with PBS and fixing in 4% paraformaldehyde for 15 min at room temperature. Cells were then washed three times for 15 min each at room temperature in PBS and permeabilized with 0.1% Triton X-100 for 5 min at 4°C. Cells were rinsed twice in PBS. An oligo dT (18)-mer, 5' end labelled with biotin (Genotex, Sigma, USA) was used as a probe for *in-situ* hybridization to poly(A)⁺ RNA. Cells were equilibrated in 2× SSC for 10 min and then subjected to hybridization at 42°C in a humidified chamber. The hybridization mixture (20 μ L) contained 80 ng oligo dT (18), 2× SSC, 1 mg/mL tRNA, 10% dextran sulphate and 25% formamide. After an overnight hybridization,

cells were washed twice in 2× SSC and once in 0.5× SSC at room temperature.

Sucrose gradient centrifugation

Cells were washed with cold (4°C) PBS and incubated in PBS containing 10 μ g/mL cycloheximide for 5 min, then harvested and centrifuged at 500xg. Cell pellets were lysed in 1 mL of ice-cold lysis buffer (140 mM KCl, 1 mM DTT, 20 mM Tris, pH 8.5, 20 mM MgCl₂, 0.5% NP-40, 0.5 U/mL RNasin) and mechanically disrupted using a 10-gauge needle. The lysates were centrifuged at 14000 g for 20 min. The final supernatant was layered onto 10 mL of 10-50% linear sucrose gradient. Centrifugation was performed at 35 000 rpm for 3 h using a Beckman Coulter SW40Ti rotor. Fractions were eluted from the top of the gradient using a BioRad fraction collector. About 200 μ L fractions were collected and OD was measured at A 260 nm to obtain the polysome profile.

Human tissue processing

All cases were provided by the MRC London Neurodegenerative Diseases Brain Bank (Institute of Psychiatry, Psychology and Neuroscience, King's College London, UK) and were collected and distributed according to local and national research ethics committee approvals (See [Supplementary Material, Table S1](#) for case details).

Western blot and immunoprecipitation

Cells were lysed in RIPA buffer, then denatured for 5 min with sample buffer. Proteins were resolved on 10% NU-PAGE Tris gels (Invitrogen). Proteins were transferred to nitrocellulose membranes using an iBlot (Invitrogen) and protein loading was assessed by Ponceau red staining. Blots were then blocked with blocking buffer (Roche) and probed using standard procedures. Immunoreactivity was detected by HRP-conjugated secondary antibodies (Sigma) and ECL kit (Promega).

For soluble and insoluble fractionation, cells were lysed in RIPA buffer and the pellet was precleared by centrifugation at 1000 g. The supernatant was centrifuged at 25 000 g. The supernatant was used for the soluble fraction and the pellet was dissolved in urea buffer for insoluble fraction. For immunoprecipitation assays, cells were grown in 10 cm diameter culture dishes until 70% confluence. The cells were stressed under A-S-R. Cells were then washed with cold PBS and lysed with IP lysis buffer. Protein A or G magnetic beads (NEB) were used for TDP-43 and HA immunoprecipitation and unconjugated magnetic bead were used for control.

Supplementary Material

[Supplementary Material](#) is available at HMG online.

Funding

The Wellcome Trust and Medical Research Council; UK Dementia Research Institute; John and Lucille Van Geest Foundation and My Name's Daddie Foundation.

References

1. Sreedharan, J., Blair, I.P., Tripathi, V.B., Hu, X., Vance, C., Rogelj, B., Ackerley, S., Durnall, J.C., Williams, K.L., Buratti,

- E. et al. (2008) TDP-43 mutations in familial and sporadic amyotrophic lateral sclerosis. *Science*, **319**, 1668–1672.
2. Neumann, M., Sampathu, D.M., Kwong, L.K., Truax, A.C., Micsenyi, M.C., Chou, T.T., Bruce, J., Schuck, T., Grossman, M., Clark, C.M. et al. (2006) Ubiquitinated TDP-43 in frontotemporal lobar degeneration and amyotrophic lateral sclerosis. *Science*, **314**, 130–133.
 3. Nishimura, A.L., Zupunski, V., Troakes, C., Kathe, C., Fratta, P., Howell, M., Gallo, J.M., Hortobágyi, T., Shaw, C.E. and Rogelj, B. (2010) Nuclear import impairment causes cytoplasmic trans-activation response DNA-binding protein accumulation and is associated with frontotemporal lobar degeneration. *Brain: J. Neurol.*, **133**, 1763–1771.
 4. Mihevc, S.P., Darovic, S., Kovanda, A., Česnik, A.B., Župunski, V. and Rogelj, B. (2016) Nuclear trafficking in amyotrophic lateral sclerosis and frontotemporal lobar degeneration. *Brain: J. Neurol.*, **140**, 13–26.
 5. Amador-Ortiz, C., Lin, W.L., Ahmed, Z., Personett, D., Davies, P., Duara, R., Graff-Radford, N.R., Hutton, M.L., Dickson, D.W. et al. (2007) TDP-43 immunoreactivity in hippocampal sclerosis and Alzheimer's disease. *Ann. Neurol.*, **61**, 435–445.
 6. Arai, T., Mackenzie, I.R.A., Hasegawa, M., Nonaka, T., Niizato, K., Tsuchiya, K., Iritani, S., Onaya, M. and Akiyama, H. (2009) Phosphorylated TDP-43 in Alzheimer's disease and dementia with Lewy bodies. *Acta Neuropathol.*, **117**, 125–136.
 7. Gliebus, G., Bigio, E.H., Gasho, K., Mishra, M., Caplan, D., Mesulam, M.M. and Geula, C. (2010) Asymmetric TDP-43 distribution in primary progressive aphasia with progranulin mutation. *Neurology*, **74**, 1607–1610.
 8. Higashi, S., Iseki, E., Yamamoto, R., Minegishi, M., Hino, H., Fujisawa, K., Togo, T., Katsuse, O., Uchikado, H., Furukawa, Y. et al. (2007) Concurrence of TDP-43, tau and alpha-synuclein pathology in brains of Alzheimer's disease and dementia with Lewy bodies. *Brain Res.*, **1184**, 284–294.
 9. Kadokura, A., Yamazaki, T., Lemere, C.A., Takatama, M. and Okamoto, K. (2009) Regional distribution of TDP-43 inclusions in Alzheimer disease (AD) brains: their relation to AD common pathology. *Neuropathology*, **29**, 566–573.
 10. Kim, S.H., Shi, Y., Hanson, K.A., Williams, L.M., Sakasai, R., Bowler, M.J. and Tibbetts, R.S. (2009) Potentiation of amyotrophic lateral sclerosis (ALS)-associated TDP-43 aggregation by the proteasome-targeting factor, ubiquitin 1. *J. Biol. Chem.*, **284**, 8083–8092.
 11. Colombrita, C., Zennaro, E., Fallini, C., Weber, M., Sommacal, A., Buratti, E., Silani, V. and Ratti, A. (2009) TDP-43 is recruited to stress granules in conditions of oxidative insult. *J. Neurochem.*, **111**, 1051–1061.
 12. Anderson, P. and Kedersha, N. (2009) Stress granules. *Curr. Biol.*, **19**, R397–R398.
 13. Kedersha, N., Chen, S., Gilks, N., Li, W., Miller, I.J., Stahl, J. and Anderson, P. (2002) Evidence that ternary complex (eIF2-GTP-tRNA(i)(Met))-deficient preinitiation complexes are core constituents of mammalian stress granules. *Mol. Biol. Cell*, **13**, 195–210.
 14. Buchan, J.R. and Parker, R. (2009) Eukaryotic stress granules: the ins and outs of translation. *Mol. Cell*, **36**, 932–941.
 15. Kedersha, N. and Anderson, P. (2009) Regulation of translation by stress granules and processing bodies. *Prog. Mol. Biol. Transl. Sci.*, **90**, 155–185.
 16. Vance, C., Scotter, E.L., Nishimura, A.L., Troakes, C., Mitchell, J.C., Kathe, C., Urwin, H., Manser, C., Miller, C.C., Hortobágyi, T. et al. (2013) ALS mutant FUS disrupts nuclear localization and sequesters wild-type FUS within cytoplasmic stress granules. *Hum. Mol. Genet.*, **22**, 2676–2688.
 17. Gasset-Rosa, F., Lu, S., Yu, H., Chen, C., Melamed, Z., Guo, L., Shorter, J., Cruz, S.D. and Cleveland, D.W. (2019) Cytoplasmic TDP-43 de-mixing independent of stress granules drives inhibition of nuclear import, loss of nuclear TDP-43, and cell death. *Neuron*, **102**, 339–357.e7.
 18. Guil, S., Long, J.C. and Caceres, J.F. (2006) hnRNP A1 relocalization to the stress granules reflects a role in the stress response. *Mol. Cell. Biol.*, **26**, 5744–5758.
 19. Kino, Y., Washizu, C., Aquilanti, E., Okuno, M., Kurosawa, M., Yamada, M., Doi, H. and Nukina, N. (2010) Intracellular localization and splicing regulation of FUS/TLS are variably affected by amyotrophic lateral sclerosis-linked mutations. *Nucleic Acids Res.*, **39**, 2781–2798.
 20. Liu-Yesucevitz, L., Bilgutay, A., Zhang, Y.J., Vanderwyde, T., Citro, A., Mehta, T., Zaarur, N., McKee, A., Bowser, R., Sherman, M. et al. (2010) Tar DNA binding protein-43 (TDP-43) associates with stress granules: analysis of cultured cells and pathological brain tissue. *PLoS One*, **5**, e13250.
 21. Tollervey, J.R., Curk, T., Rogelj, B., Briese, M., Cereda, M., Kayikci, M., Konig, J., Hortobágyi, T., Nishimura, A.L., Zupunski, V. et al. (2011) Characterizing the RNA targets and position-dependent splicing regulation by TDP-43. *Nat. Neurosci.*, **14**, 452–458.
 22. Klim, J.R., Williams, L.A., Limone, F., Juan, I.G.S., Davis-Dusenbery, B.N., Mordes, D.A., Burberry, A., Steinbaugh, M.J., Gamage, K.K., Kirchner, R. et al. (2019) ALS-implicated protein TDP-43 sustains levels of STMN2, a mediator of motor neuron growth and repair. *Nat. Neurosci.*, **22**, 167–179.
 23. Dormann, D., Rodde, R., Edbauer, D., Bentmann, E., Fischer, I., Hruscha, A., Than, M.E., Mackenzie, I.R.A., Capell, A., Schmid, B. et al. (2010) ALS-associated fused in sarcoma (FUS) mutations disrupt transportin-mediated nuclear import. *EMBO J.*, **29**, 2841–2857.
 24. Anderson, E.N., Gochenaour, L., Singh, A., Grant, R., Patel, K., Watkins, S., Wu, J.Y. and Pandey, U.B. (2018) Traumatic injury induces stress granule formation and enhances motor dysfunctions in ALS/FTD models. *Hum. Mol. Genet.*, **27**, 1366–1381.
 25. Zhang, K., Daigle, J.G., Cunningham, K.M., Coyne, A.N., Ruan, K., Grima, J.C., Bowen, K.E., Wadhwa, H., Yang, P., Rigo, F. et al. (2018) Stress granule assembly disrupts nucleocytoplasmic transport. *Cell*, **173**, 958–971.e17. doi: [10.1016/j.cell.2018.03.025](https://doi.org/10.1016/j.cell.2018.03.025).
 26. Khalfallah, Y., Kuta, R., Grasmuck, C., Prat, A., Durham, H.D. and Velde, C.V. (2018) TDP-43 regulation of stress granule dynamics in neurodegenerative disease-relevant cell types. *Sci. Rep.*, **8**, 7551–7513.
 27. Hock, E.-M., Maniecka, Z., Hruska-Plochan, M., Reber, S., Laferrière, F., SSM, K., Ederle, H., Gittings, L., Pelkmans, L., Dupuis, L. et al. (2018) Hypertonic stress causes cytoplasmic translocation of neuronal, but not astrocytic, FUS due to impaired transportin function. *Cell Rep.*, **24**, 987–1000.e7.
 28. Zhang, Y.-J., Gendron, T.F., Ebbert, M.T.W., O'Raw, A.D., Yue, M., Jansen-West, K., Zhang, X., Prudencio, M., Chew, J., Cook, C.N. et al. (2018) Poly(GR) impairs protein translation and stress granule dynamics in C9orf72-associated frontotemporal dementia and amyotrophic lateral sclerosis. *Nat. Med.*, **24**, 1136–1142.
 29. Moisse, K., Mephram, J., Volkening, K., Welch, I., Hill, T. and Strong, M.J. (2009) Cytosolic TDP-43 expression following axotomy is associated with caspase 3 activation in NFL^{-/-} mice: support for a role for TDP-43 in the

- physiological response to neuronal injury. *Brain Res.*, **1296**, 176–186.
30. Volkening, K., Leystra-Lantz, C., Yang, W., Jaffee, H. and Strong, M.J. (2009) Tar DNA binding protein of 43 kDa (TDP-43), 14-3-3 proteins and copper/zinc superoxide dismutase (SOD1) interact to modulate NFL mRNA stability. Implications for altered RNA processing in amyotrophic lateral sclerosis (ALS). *Brain Res.*, **1305**, 168–182.
 31. Wang, I.F., Wu, L.S., Chang, H.Y. et al. (2008) TDP-43, the signature protein of FTL-D-U, is a neuronal activity-responsive factor. *J. Neurochem.*, **105**, 797–806.
 32. Higashi, S., Kabuta, T., Nagai, Y., Tsuchiya, Y., Akiyama, H. and Wada, K. (2013) TDP-43 associates with stalled ribosomes and contributes to cell survival during cellular stress. *J. Neurochem.*, **126**, 288–300.
 33. Neelagandan, N., Gonnella, G., Dang, S., Janiesch, P.C., Miller, K.K., Kuchler, K., Marques, R.F., Indenbirken, D., Alawi, M., Grundhoff, A. et al. (2018) TDP-43 enhances translation of specific mRNAs linked to neurodegenerative disease. *Nucleic Acids Res.*, **47**, gky972.
 34. Cougot, N., Babajko, S. and Seraphin, B. (2004) Cytoplasmic foci are sites of mRNA decay in human cells. *J. Cell Biol.*, **165**, 31–40.
 35. Fontana, F., Siva, K. and Denti, M.A. (2015) A network of RNA and protein interactions in fronto temporal dementia. *Front. Mol. Neurosci.*, **8**, 9.
 36. Al-Chalabi, A., Calvo, A., Chio, A., Colville, S., Ellis, C.M., Hardiman, O., Heverin, M., Howard, R.S., Huisman, M.H.B., Keren, N. et al. (2014) Analysis of amyotrophic lateral sclerosis as a multistep process: a population-based modelling study. *Lancet Neurol.*, **13**, 1108–1113.